J Mater Sci: Mater Med
DOI 10.1007/s10856-013-4902-9

Biocompatibility studies of low temperature nitrided and collagen-I coated AISI 316L austenitic stainless steel

M. Martinesi · M. Stio · C. Treves · F. Borgioli

Received: 2 October 2012 / Accepted: 23 February 2013

Abstract The biocompatibility of austenitic stainless steels can be improved by means of surface engineering techniques. In the present research it was investigated if low temperature nitrided AISI 316L austenitic stainless steel may be a suitable substrate for bioactive protein coating consisting of collagen-I. The biocompatibility of surface modified alloy was studied using as experimental model endothelial cells (human umbilical vein endothelial cells) in culture. Low temperature nitriding produces modified surface layers consisting mainly of S phase, the supersaturated interstitial solid solution of nitrogen in the austenite lattice, which allows to enhance surface microhardness and corrosion resistance in PBS solution. The nitriding treatment seems to promote the coating with collagen-I, without chemical coupling agents, in respect of the untreated alloy. For biocompatibility studies, proliferation, lactate dehydrogenase levels and secretion of two metalloproteinases (MMP-2 and MMP-9) were determined. Experimental results suggest that the collagen protection may be favourable for endothelial cell proliferation and for the control of MMP-2 release.

1 Introduction

The main problem of metallic implant materials, such as austenitic stainless steels, is the decrease or the lack of biocompatibility, due mainly to the toxic effects of metal release from implants into body fluids [1]. Austenitic stainless steels have high corrosion resistance, due to the formation on their surface of a passive film, mainly consisting of chromium oxide, which gives very good corrosion resistance and allows to form a barrier between the alloy and the surrounding medium [2]. However, in contact with body fluids these alloys tend to corrode, limiting their clinic use [3]. The metallic corrosion products may be associated with allergic responses [4], and, in addition, the degradative process of the implant may reduce its structural integrity [5]. AISI 316L stainless steel and its derivatives, and nitinol, a nickel–titanium alloy, are widely used for stents, which are tubular meshes, applied as cardiovascular devices when a partial or complete occlusion (stenosis) of the vessels, in particular the small vessels supplying blood to the cardiac muscle, develops [6]. The poor biocompatibility of these metal devices may be due not only to the corrosion of the alloys with the release of potentially toxic metal ions, but also to unwanted side effects, such as the activation of the coagulation cascade with the development of thrombus, and the accumulation of inflammatory cells in the space separating the endothelial cell layer (intima) from the smooth muscle cell layer (media) with the risk of a partial or complete occlusion (stenosis) of the vessel, due also to the proliferation of vascular smooth muscle cells of the vessel walls. It has been shown that titanium is much more thrombogenic than other commonly used biomaterials such as stainless steel [7]. Santin et al. [6] demonstrated that stainless steel activates both platelets and macrophages, which release pro-inflammatory cytokines and growth factors with the risk of a protracted inflammation and consequent restenosis. One of the factors contributing to the reocclusion at the site of intravascular stent placement is injury and also loss of the endothelium. Intact

M. Martinesi · M. Stio · C. Treves
Department of Biomedical, Experimental and Clinical Sciences, University of Florence, Viale Morgagni 50, 50134 Florence, Italy

F. Borgioli (✉)
Department of Industrial Engineering, University of Florence, Via S. Marta 3, 50139 Florence, Italy
e-mail: francesca.borgioli@unifi.it

Published online: 08 March 2013

endothelium plays in fact an integral part in maintaining vascular homeostasis and normal function, being associated with reduced restenosis [8], as it represents a dynamic physiological endothelialization border between the circulating blood and the surrounding tissue. Moreover, it is well known that native endothelium plays a critical role in controlling the function of the human cardiovascular system, being also involved in regulating vascular tone and orchestrating the immune response. Therefore, it is very important that a rapid re-endothelialization of the arterial wall and endothelialization of the intravascular stent surface after implantation occur [9], avoiding, on the other hand, the excessive proliferation of vascular smooth muscle cells, as this plays a key role in arterial occlusion. Yeh et al. [10] observed that AISI 316L stainless steel and nitinol, commonly used to make vascular stents, inhibit the growth of endothelial cells during re-endothelialization. It is therefore of fundamental importance to find a surface treatment and/or coating in order to accelerate the process of re-endothelialization and eliminate any potential endothelial dysfunction, as intact endothelium is associated with reduced restenosis [8, 11]. For this purpose, Yuan et al. [9] used a poly *n*-butyl methacrylate coating, and demonstrated a significant increase in the attachment and proliferation of endothelial cells and a reduction in the platelet adhesion, compared with those on the uncoated AISI 316L stainless steel. In order to improve the biocompatibility of coronary stents and to enhance endothelialization, so reducing the danger of restenosis, Waterhouse et al. [12] have proposed the immobilization of recombinant human tropoelastin on AISI 316L stainless steel using a plasma-activated coating. Many other modifications have been suggested in order to modulate the interface properties of the implanted biomaterials, as coating or grafting adhesive proteins that mediate cellular attachment, such as fibronectin, laminine, collagen and peptides [13, 14], since there is evidence that pre-adsorbed proteins on interfaces may improve blood and tissue compatibility [15–17]. Moreover, the cellular attachment to the implant surface depends, almost in part, on the proteins adsorbed to the surface from the serum present in the culture medium, in in vitro experiments, or secreted by the cells. In particular, collagen, a fibrous protein, which is the major component of mammalian connective tissue, is involved in many biological functions as cell attachment and tissue regeneration, and it is expected that it may represent a support for cell adhesion, providing rapid coverage with protective endothelial cells. Hauser et al. [18] demonstrated that the cell viability and cell attachment rate on the plasma pre-treated, collagen coated surfaces of titanium and stainless steel implants were significantly increased compared to the non coated surfaces, ameliorating therefore the biocompatibility of implant materials in vitro. Chen et al. [19, 20] applied a collagen/heparin multilayer coating on titanium surface, and observed that this coating has the ability to maintain cell viability, showing also good biocompatibility in vitro.

The presence of a coating on the surface of alloys used for implants, like stainless steels and titanium alloys, may influence the corrosion resistance of these materials. When a coating strategy with bioactive proteins is chosen for the metallic implant, the imperfect coverage of the surface or poor adhesion by the proteins may cause a local concentration increase of body fluids components, like chloride ions, so that localised corrosion phenomena more easily may occur. Corrosion resistance of alloy substrate can be enhanced by surface engineering techniques, which modify the characteristics of the surface layers [21]. Regarding austenitic stainless steels, low temperature nitriding has been shown to markedly increase the corrosion resistance of these materials in chloride-ion containing solutions, so that both pitting and crevice phenomena are reduced [2, 22–24]. When this treatment is applied, a modified surface layer forms, which consists mainly of a metastable phase, known as S phase or expanded austenite, which can be outlined as a supersaturated interstitial solid solution of nitrogen (up to $\sim$10 wt%) in the expanded and distorted austenite lattice [2, 22, 23].

The aim of the present research was to investigate if low temperature nitrided AISI 316L austenitic stainless steel may be a suitable substrate for bioactive protein coating consisting of collagen-I, and to study the biocompatibility of the surface modified alloy using as experimental model endothelial cells (HUVEC, human umbilical vein endothelial cells) in culture. The microstructural, mechanical, corrosion resistance and water wettability characteristics of the nitrided samples were studied and were compared with those of the untreated alloy. Collagen coating was carried out following the procedure reported by Hauser et al. [18], without the use of chemical coupling agents. For biocompatibility tests, HUVEC were cultured in contact with the samples under study, i.e. nitrided or not and collagen coated or not AISI 316L austenitic stainless steel. Cell proliferation and extracellular and intracellular lactate dehydrogenase (LDH) levels were determined. Moreover, it was stated to investigate on the activity of two matrix metalloproteinases (MMPs), MMP-2 and MMP-9. MMPs represent a group of over 25 enzymes, which play an important role in extracellular matrix degradation [25]. In particular, MMP-2 and MMP-9, known as gelatinases, can degrade different substrates, which are major components of vascular basal lamina [26]. MMP-2 and MMP-9, which are ubiquitous in the heart, have emerged as important players in many cardiovascular diseases [27]. In the present study, we have investigated whether the low temperature nitriding and collagen coating of AISI 316L stainless steel

could modulate the production of MMPs from HUVEC in response to interactions with such samples.

2 Materials and methods

2.1 Preparation of AISI 316L samples

The material used in the present study was AISI 316L austenitic stainless steel with the following chemical composition (in wt%): 0.029 C, 16.6 Cr, 10.3 Ni, 2.01 Mo, 0.90 Mn, 0.34 Si, 0.001 S, 0.029 P. The steel was in the form of cold rolled, annealed and pickled plates. Prismatic samples (40 × 17 × 0.7 mm) were obtained by cutting and then were ground and polished up to 6-μm diamond suspension. The average surface roughness R_a (arithmetical mean deviation of the roughness profile from the mean line) was 0.03 μm.

X-ray diffraction analysis of the untreated steel shows that, besides γ-Fe (f.c.c.) peaks, very small peaks of b.c.t. martensite (α'), formed during grinding and polishing, are observed; the martensite peaks overlap the peaks of α-Fe (b.c.c.), which may be also present.

Glow-discharge nitriding treatment was performed in a laboratory plasma equipment, previously described [28]. Before the nitriding treatment the samples were heated up to about 330 °C by means of a cathodic sputtering performed at 1.3 hPa with 80 vol% N_2 and 20 vol% H_2; after the sputtering step the pressure and the temperature were increased up to their nominal values. The treatment was performed at 400 °C, for 5 h, at pressure of 5 hPa, using a gas composition of 80 vol% N_2 and 20 vol% H_2. The current density during the treatment was 1.6 mA/cm^2 and the voltage drop was 195 V.

2.2 Microstructural and mechanical characterization

The microstructure of untreated and treated samples was examined by optical and scanning electron microscopies and energy dispersion spectroscopy (EDS) analysis techniques. X-ray diffraction analysis (Cu Kα radiation) was carried out in order to identify the phases present in the surface layers. Diffraction patterns were collected in glancing angle configuration, with constant incident angles in the range 5–15°, and in Bragg–Brentano configuration; the patterns were analysed by means of the program MAUD using the Rietveld method [29].

Surface microhardness measurements (Knoop indenter, 25 and 50 gf) were carried out on the samples. Roughness measurements were performed on the surface of the samples before and after the nitriding treatment by using a stylus profilometer tester (track length: 4.8 mm).

2.3 Corrosion tests

Corrosion resistance of untreated and nitrided samples was studied in aerated phosphate-buffered saline (PBS) solution at room temperature. PBS, from Sigma, contained 137 mM NaCl, 2.7 mM KCl, 4.3 mM $NaH_2PO_4{\cdot}7H_2O$ and 1.4 mM KH_2PO_4. A three-electrode electrochemical flat cell equipped with an Ag/AgCl reference electrode (3.5 M KCl) and a platinum grid as a counterelectrode was used for all the tests. The sample surface area exposed to the electrolyte was 1 cm^2.

Polarisation measurements were performed potentiodynamically at sweep rate of 0.3 mV/s after a delay period of 20 h. Three corrosion tests for each sample type were carried out in order to assess the result.

Electrochemical impedance spectroscopic (EIS) measurements were performed at open circuit potential (OCP) after a delay period of 20 h. The frequency range was between 40 kHz and 25 mHz with data density of 10 points per decade and an *ac* amplitude (rms) of 10 mV. EIS spectra were modelled using non linear least square analysis software (Gamry EIS300).

2.4 Contact angle measurements

The water wettability of untreated and nitrided samples was determined by sessile drop method. Before measurements the samples were prepared in two different ways: one set of samples (untreated and nitrided) was sonicated in acetone for 5 min and then dried in air; the other set of samples (untreated and nitrided) was subjected to sterilization procedure and then was incubated with acetic acid used at the same concentration present in the collagen solution (see next sections) and subjected to the same procedure followed for the collagen coating.

Water wettability was evaluated using distilled water as probe liquid, and the volume of the drops was fixed at 3 μl. All the measurements were carried out at room temperature. The static water contact angle was determined as the mean of at least ten independent measurements.

2.5 Sterilization

For the sterilization procedure, the untreated and nitrided AISI 316L samples were first rinsed one time with 100 % ethanol (30 min), and repeatedly washed with sterilized deionized water. The samples were then exposed overnight to UV irradiation.

2.6 Collagen coating procedure

Half of the samples (untreated and nitrided) were collagen coated, according to the procedure reported by Hauser et al.

[18]. Collagen type I from rat tail 4 mg/ml in 20 mM acetic acid (BD Biosciences, Bedford, MA) was diluted 1:8 with sterilized deionized water to 0.5 mg/ml end concentration. The samples were incubated with 0.5 ml diluted collagen/cm^2 for 24 h at 4 °C under sterile conditions. Afterwards the supernatant was discarded and the samples were incubated with 0.5 ml diluted collagen/cm^2 for another 48 h at 37 °C under sterile conditions. After drying, the samples were rinsed with sterilized deionized water to eliminate the non adherent collagen. The samples which were not collagen coated were incubated with acetic acid used at the same concentration present in the collagen solution and were subjected to the same procedure followed for the collagen coating. The untreated stainless steel samples were indicated as S, the nitrided ones as T. When these samples were collagen coated, they were indicated as SC and TC, respectively.

2.7 Cell cultures

Normal HUVEC cryopreserved at the end of the primary culture were obtained by Merck Millipore. HUVEC were negative for bacteria and fungal growth. HUVEC were grown in EndoGRO-LS-medium (containing EndoGRO-LS Supplement), obtained by Merck Millipore. The final concentration of the components in the supplemented medium were: human epidermal growth factor (rh EGF), 5 ng/ml; ascorbic acid, 50 μg/ml; L-glutamine, 10 mM; hydrocortisone hemisuccinate, 1.0 μg/ml; heparin sulfate, 0.75 U/ml; foetal bovine serum (FBS), 2 % v/v. Cultures were maintained at 37 °C in humidified atmosphere containing 5 % CO_2. According to the suggestions of Kalogeris et al. [30], we used HUVEC not over passage five. When the cells were at 70 % confluence, the cultures were divided in groups, each containing 5×10^4 cells for the experiments after 3 days, and 2×10^4 cells for the experiments after 5 days, in order to obtain, at the end of the incubation period, about 80 % confluence. Control group was represented by cells that received only complete culture medium; four groups, obtained by seeding the HUVEC on the metallic samples under study, were maintained in direct contact with the four sample types (one sample type for each group) for 4 h or 3 or 5 days, depending on the experiments.

2.8 Proliferation studies

The WST-8 Cell Proliferation Assay Kit (Cayman Chemical Company) was used to assess cell proliferation and viability. The assay is based on the extracellular reduction of WST-8 by NADH produced in the mitochondria via trans-plasma membrane electron transport and an electron mediator. WST-8 produces a water-soluble formazan which dissolves directly into the culture medium, eliminating the need for an additional solubilization step. The detection sensitivity is higher than that for other tetrazolium salts. The formazan dye produced by viable cells was quantified by measuring the absorbance of the dye solution at 450 nm. Background absorbance of the culture medium without cells was subtracted. Proliferation was determined both on HUVEC present in the well and on the cells present on the surface of each sample, after different incubation times (4 h, 3 or 5 days). Proliferation was expressed as per cent of the proliferation registered when the cells were put in contact with the untreated non collagen coated samples (S).

2.9 Lactate dehydrogenase assay

The LDH Cytotoxicity Assay Kit (Cayman Chemical Company) was used to assess the amount of LDH released by HUVEC into the culture medium as a result of cytotoxicity (extracellular LDH) and the amount of LDH present in cell lysates (intracellular LDH). The cells were incubated for 3 days with culture medium alone (control group) or with the samples under study. This kit uses a coupled two-step reaction. In the first step, LDH catalyzes the reduction of NAD^+ to NADH and H^+ by oxidation of lactate to pyruvate. In the second step of the reaction, diaphorase uses NADH and H^+ to catalyze the reduction of a tetrazolium salt to formazan, which absorbs at 490 nm. LDH activity was expressed as μU/ml.

2.10 Zymography

ProMMP-2, MMP-2, proMMP-9 and MMP-9 gelatinase activities were visualised by zymography. Briefly, SDS polyacrylamide gels (8 %) containing 0.1 % gelatine were overlaid with 4 % stacking gels. Sample supernatants were mixed (10:1 volume) with a sample buffer consisting of 50 mM Tris-HCl, pH 6.8, 2 % SDS, 20 % glycerol, and 0.03 % bromophenol blue. After loading the samples, electrophoresis was carried out at 125 V for 2 h. After electrophoresis, the gels were soaked in 2.5 % Triton X-100 on a shaker for 1 h, at room temperature, changing the solution after 30 min, to eliminate SDS. The gels were then equilibrated for 30 min with the digestion buffer (50 mM Tris–HCl, pH 7.5, 5 mM $CaCl_2$, 200 mM NaCl) at room temperature with gentle agitation, then replaced with fresh digestion buffer and incubated at 37 °C overnight. The gels were then stained for 1–2 h with 0.5 % Coomassie Brilliant Blue in 30 % methanol and 10 % acetic acid and destained with 30 % methanol and 10 % acetic acid, after which clear bands of digested gelatine were well visible. In order to obtain densitometric data the gels were scanned by Chemi-Doc (Bio-Rad), utilising the

Quantity One program (Bio-Rad). MMPs levels measured in the culture medium were normalized with basis on cell proliferation.

2.11 Statistical methods

Statistical significance was determined by either one-way analysis of variance (ANOVA), followed by Bonferroni *t* test or by Student's *t* test. One-way ANOVA was used to determine significance among groups, after which the modified *t* test with the Bonferroni correction was used for comparison between individual groups. Differences were considered significant at $P < 0.05$.

3 Results

3.1 Morphology and microstructure of the nitrided samples

On AISI 316L austenitic stainless steel low temperature glow-discharge nitriding process produces modified surface layers. After the treatment the surface of the samples shows an etched appearance, as observed also in our previous papers [24, 28] and by other authors [31, 32] (Fig. 1a). This peculiar morphology can be ascribed to both cathodic sputtering and the treatment itself. In fact, the presence of slip bands within the austenitic grains, as delineated by plasma etching, and high reliefs at grain boundaries suggests that the formation of the modified surface layers is accompanied by high stresses which cause local plastic deformation. As a consequence, a slight increase of surface roughness ($R_a = 0.07 \pm 0.01$ μm) is observed.

The typical cross-section microstructure of the modified surface layers is shown in Fig. 1b. A double layer microstructure is delineated by chemical etching with glyceregia, and it consists of a thicker outer layer and a thinner inner layer, separated one from the other and from the substrate by strong etched lines. As also observed previously [24, 28], in the outer layer few slip bands are delineated. In the modified layers the grain boundaries appear as the continuation of the austenite matrix grain boundaries, suggesting that the layers are essentially a modification of the austenite matrix, as reported also in previous papers [24, 28].

According to X-ray diffraction analysis (Fig. 2), the outer modified layer consists mainly of the so-called S phase, the supersaturated interstitial solid solution of nitrogen in the expanded and distorted f.c.c. lattice. Small amounts of nitrogen induced h.c.p. martensite, ε'_N, are also observed. As the X-ray beam penetrates more deeply in the layers, small peaks ascribable to a solid solution of nitrogen in γ-Fe, γ(N) (f.c.c.), and to the γ-Fe substrate are

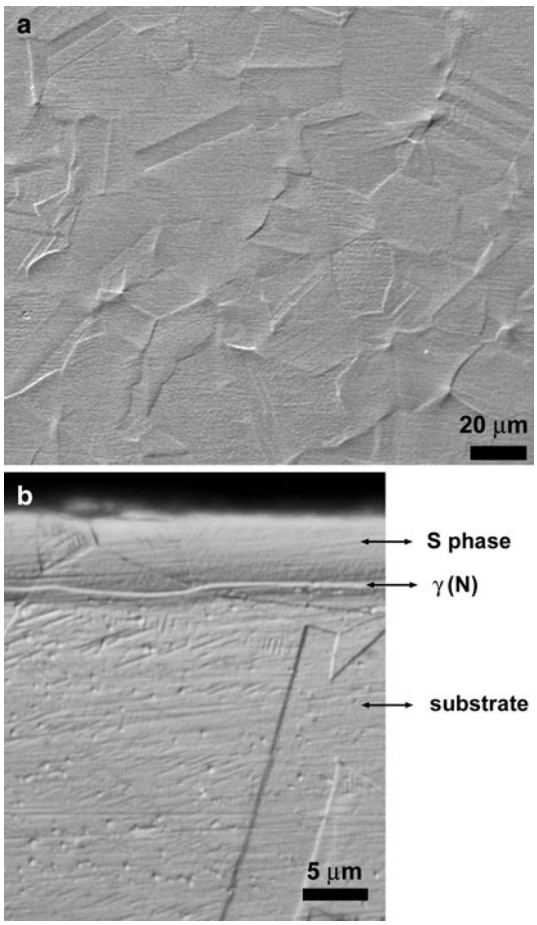

Fig. 1 Surface morphology (**a**) and cross-section microstructure of the modified layers (etchant: glyceregia) (**b**) of an AISI 316L stainless steel sample nitrided at 400 °C, at 5 hPa for 5 h

detected. It may be hypothesised that γ(N) is present in the inner modified layer, as also previously observed [24].

The thickness of the modified layers is 7 ± 1 μm as a whole.

3.2 Surface microhardness

The low temperature nitriding treatment is able to markedly increase surface microhardness of the untreated alloy. Microhardness values of untreated and nitrided AISI 316L samples are reported in Table 1. The marked decrease of hardness values observed for nitrided samples as the indenter load increases may be ascribed not only to the indentation size effect, but also to the fact that with a greater load deeper regions with lower nitrogen content are detected.

3.3 Corrosion behaviour

Corrosion resistance of AISI 316L steel is enhanced by low temperature nitriding. An example of polarisation curves

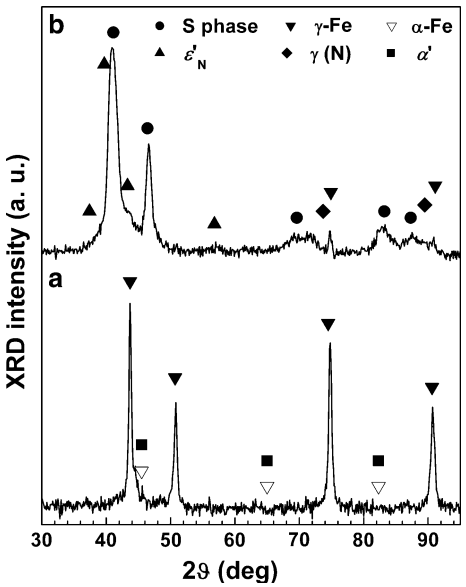

Fig. 2 X-ray diffraction patterns of untreated (**a**) and nitrided (**b**) AISI 316L stainless steel samples

Table 1 Surface Knoop microhardness values of untreated and nitrided AISI 316L stainless steel samples (indenter loads: 25 and 50 gf)

Sample type	Microhardness (HK)	
	Load 25 gf	Load 50 gf
Untreated	220 ± 6	194 ± 4
Nitrided	1360 ± 40	820 ± 30

recorded for untreated and nitrided samples tested in PBS are shown in Fig. 3. The corrosion behaviour of both sample types is characteristic of a passive material subjected to localised corrosion when the potential is higher than a threshold. Nitrided samples have a corrosion potential value of −20 mV (Ag/AgCl), approximately 150 mV higher than that of the untreated samples, while their passive current values are up to 25 times lower. At about +1,130 mV (Ag/AgCl) both sample types show a passive–transpassive transition and their anodic currents markedly increase, but beyond approximately +1,310 mV (Ag/AgCl) the anodic current density values of the nitrided samples are lower than those of the untreated ones.

Electrochemical impedance spectroscopy (EIS) provides information on charge transfer and mass transport processes occurring at the electrolyte/electrode interface and in the passive oxide film. The typical EIS spectra of the untreated and nitrided samples tested in PBS at the respective OCP values are shown in Fig. 4; the data are presented in the form of Nyquist (a) and Bode (phase angle) (b) plots. A physical picture of the corrosion behaviour of the system can be obtained modelling the EIS

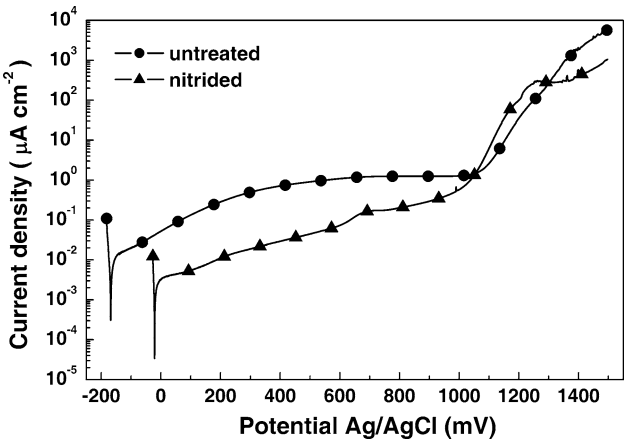

Fig. 3 Polarisation curves of untreated and nitrided AISI 316L stainless steel samples (*solution*: PBS, aerated)

data with an appropriate electrical equivalent circuit (EEC). EIS data of austenitic stainless steels put in contact with many solutions are usually modelled using an EEC describing the behaviour of processes characterized by a high frequency (HF) time constant, assigned to the oxide-electrolyte interface, and a low frequency (LF) time constant, assigned to the redox processes occurring in the passive layer [33, 34]. However, in the present study it was chosen to model EIS spectra with the HF time constant only, since the LF time constant element could not be clearly defined. This simplified EEC model was used also by other authors for modelling EIS spectra of austenitic stainless steels [35–37]. Even with only one time constant, the agreement between the experimental (circles and triangles) and modelled (solid line) data was good. The EEC used is shown as an inset in Fig. 4a; the EEC parameter values obtained by fitting experimental data are reported in Table 2. The electronic elements have the following meanings: R_e is the electrolyte resistance between the working and the reference electrode, R_{ct} is the charge transfer resistance, related to the rate of corrosion reaction at OCP, and CPE represents the double layer/space charge capacitance, related to charging/discharging processes. A better agreement between theoretical and experimental data is obtained if a pure capacitance is replaced with a constant phase element (CPE), owing to a distribution of relaxation times as a result of inhomogeneities present at the micro or nano (atomic or molecular) level, such as surface roughness/porosity, adsorption or diffusion [38]. The impedance of a CPE is defined as:

$$Z = [\text{CPE } (i\omega)^n]^{-1}$$

where CPE is a constant parameter, ω is the angular frequency, $i^2 = -1$ is the imaginary number, and n is the CPE exponent. Depending on n, CPE can represent a pure capacitance ($n = 1$), a pure resistance ($n = 0$), a pure

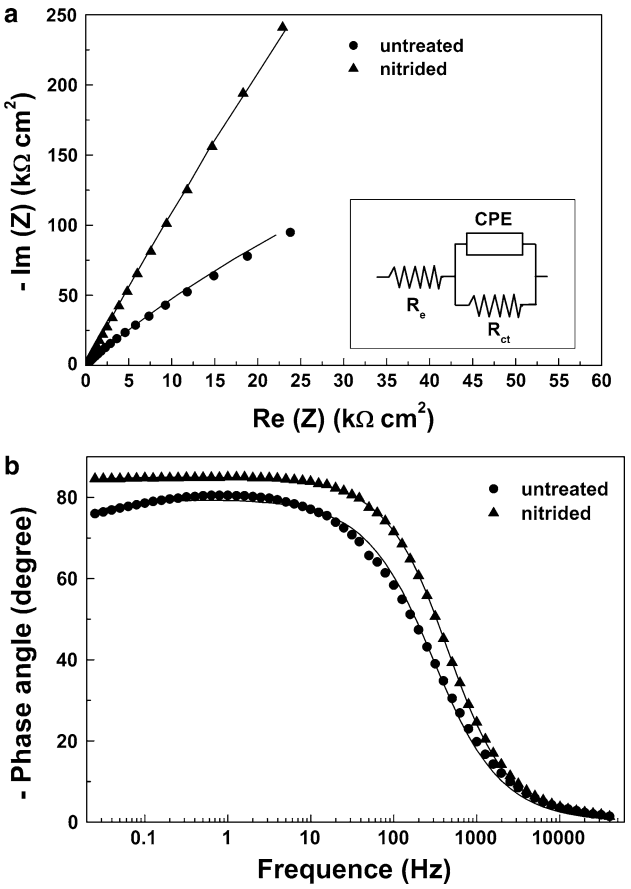

Fig. 4 Nyquist (**a**) and Bode (phase) (**b**) plots of untreated and nitrided AISI 316L stainless steel samples, recorded at the respective OCP values (*solution*: PBS, aerated). *Symbols* Experimental data, *lines* the modelled data obtained using the equivalent electrical circuit shown in the *inset* of "**a**"

inductance ($n = -1$), or a Warburg impedance, i.e. a mass transport related impedance ($n = 0.25$–0.5). The deviation of n from these values indicates a deviation from the ideal behaviour of the system.

The analysis of EIS data shows that for both sample types a deviation from pure capacitance of the double layer occurs. Moreover, low temperature nitrided samples show a greater charge transfer resistance in comparison with untreated samples, in accordance with the higher corrosion resistance shown by this sample type.

3.4 Water wettability

Water wettability evaluation shows that after sonication in acetone the contact angle of untreated AISI 316L is fairly high, $72.8 \pm 0.7°$. After low temperature nitriding the contact angle significantly increases up to $82.0 \pm 0.5°$, suggesting a more hydrophobic behaviour.

When the samples are subjected to sterilization procedure and incubated in acetic acid solution, as the collagen coated samples, the contact angle of untreated samples is $72.5° \pm 0.7°$, comparable with the value obtained for the same sample type after sonication in acetone. On the other hand, the contact angle of the nitrided samples decreases up to $71.0° \pm 0.8°$, reaching slightly lower values than those of the untreated steel. It may be hypothesised that the sterilization and acetic acid incubation procedures are able to modify the surface condition of the nitrided samples.

3.5 Collagen coating

Surface morphology of untreated and nitrided AISI 316L samples subjected to collagen-I coating is shown in Fig. 5. The untreated samples show a poor surface coverage by collagen (Fig. 5a), while on nitrided samples a better adhesion is observed, and large regions covered by collagen are present (Fig. 5b).

3.6 HUVEC proliferation

The influence of untreated and nitrided AISI 316L samples, subjected or not to collagen coating, on HUVEC proliferation was investigated. In particular, the determination of cell proliferation was carried out on both HUVEC proliferating in the wells (Table 3) and HUVEC proliferating directly on the samples (Table 4). HUVEC proliferation was determined after 4-h or 3- or 5-day incubation. The data were calculated setting the value obtained in the presence of samples S equal to 100.

Considering HUVEC proliferating in the wells, after 4 h no significant differences are observed among the different groups (data not shown). After 3 days no significant difference in HUVEC proliferation is registered among the different groups (Table 3), while, after 5 days, it may be observed that the collagen coating (i.e. the presence of SC and TC samples) induces significantly higher proliferation values if compared with those obtained in the presence of the untreated samples (S).

On the other hand, when the proliferation of HUVEC present on the surface of the samples was studied, after 3- or 5-day incubation a remarkable difference between the untreated and collagen uncoated samples (S) and the other samples is always registered (Table 4). After 4-h incubation, the proliferation values are very low or undetectable (data not shown). Cell proliferation is significantly higher in comparison with S, after 3- or 5- day incubation with the samples T or SC or TC. Moreover, after 3 days, HUVEC proliferation on the collagen coated samples (SC and TC) is higher in comparison with that registered in the presence of samples T, while, after 5 days, cell proliferation is significantly higher when the cells were put in contact with the nitrided and collagen coated samples (TC) in comparison with the values obtained in the presence of the samples T

Table 2 Best fitting EEC parameter values for EIS spectra of untreated and nitrided AISI 316L stainless steel samples tested in PBS at the respective OCP (model: see inset of Fig. 4a)

Sample type	R_e (Ω cm^2)	R_{ct} (MΩ cm^2)	CPE $\times$ 10^5 (Ω^{-1} s^n cm^{-2})	n
Untreated	23.8 $\pm$ 0.2	1.7 $\pm$ 0.2	5.3 $\pm$ 0.1	0.89 $\pm$ 0.1
Nitrided	23.2 $\pm$ 0.2	21 $\pm$ 2	2.4 $\pm$ 0.1	0.95 $\pm$ 0.1

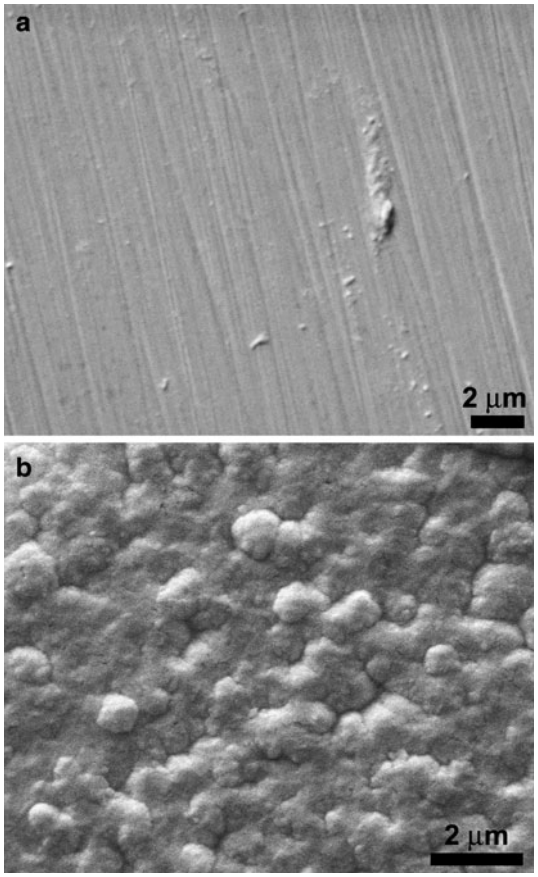

Fig. 5 Surface morfology of untreated (**a**) and nitrided (**b**) AISI 316L stainless steel samples after collagen-I coating procedure

Table 3 Effect of AISI 316L stainless steel sample types on the proliferation of HUVEC present in the well

Sample type	3-Day proliferation	5-Day proliferation
T	87 $\pm$ 13	131 $\pm$ 28
SC	92 $\pm$ 4	150 $\pm$ 4*
TC	92 $\pm$ 3	138 $\pm$ 16**

Cells were put in contact for 3 or 5 days with samples (*S* untreated stainless steel, *T* nitrided stainless steel, *SC* untreated, collagen coated stainless steel, *TC*, nitrided, collagen coated stainless steel). Data are given relative to the values obtained in the presence of samples S, set equal to 100. Each value represents the mean $\pm$ SD of five (3 days) or three (5 days) separate experiments, each performed in triplicate

* $P < 0.01$ (in comparison with S); ** $P < 0.05$ (in comparison with S)

Table 4 Effect of AISI 316L stainless steel sample types on the proliferation of HUVEC present on the surface of the samples

Sample type	3-Day proliferation	5-Day proliferation
T	115 $\pm$ 7**	167 $\pm$ 4*
SC	134 $\pm$ 5*,°	174 $\pm$ 3*
TC	136 $\pm$ 9*,°	219 $\pm$ 4*,^

Cells were put in contact for 3 or 5 days with samples (*S* untreated stainless steel, *T* nitrided stainless steel, *SC* untreated, collagen coated stainless steel, *TC* nitrided, collagen coated stainless steel). Data are given relative to the values obtained in the presence of samples S, set equal to 100. Each value represents the mean $\pm$ SD of five (3 days) or three (5 days) separate experiments, each performed in triplicate

* $P < 0.01$ (in comparison with S); ** $P < 0.05$ (in comparison with S); ° $P < 0.01$ (in comparison with T); ^ $P < 0.01$ (in comparison with T and SC)

and SC. The highest proliferation values are registered when HUVEC were cultured in the presence of TC for 5 days.

3.7 Extracellular and intracellular lactate dehydrogenase levels

Lactate dehydrogenase is a soluble enzyme located in the cytosol, which is released into the surrounding culture medium upon cell damage or lysis. Therefore, LDH activity in the culture medium can be used as an indicator of cell membrane integrity, representing a measurement of cytotoxicity. In order to verify whether the contact of HUVEC with the samples under study may influence not only LDH release but also LDH levels present in the cells, the activity of this enzyme was determined after 3-day incubation in both the culture medium (extracellular LDH) and cell lysates (intracellular LDH). In Table 5 the results obtained by the determination of extracellular and intracellular LDH levels are reported as µU/ml, together with intracellular/extracellular (intra/extra) LDH ratio. The contact with the samples always induces a significantly higher release of LDH (extracellular LDH) in comparison with control HUVEC (H), i.e. cells maintained in the presence of the culture medium alone. In the presence of the nitrided and collagen coated samples (TC), LDH release is lower than in the presence of the untreated, collagen coated or not samples (S and SC), while LDH

Table 5 Effect of AISI 316L stainless steel sample types on lactate dehydrogenase (LDH) activity assayed in the culture medium (extracellular LDH) or in cell lysates (intracellular LDH) of HUVEC

	Extra LDH (μU/ml)	Intra LDH (μU/ml)	Intra/extra
H	38.6 ± 3.5	258.3 ± 10.0	6.69 ± 0.65
S	54.7 ± 3.7*	237.1 ± 15.0	4.33 ± 0.40*
T	48.5 ± 3.2*	227.3 ± 14.0**	4.68 ± 0.42*
SC	54.5 ± 4.0*	224.3 ± 8.3*	4.11 ± 0.33*,^
TC	48.4 ± 3.3*,°	222.6 ± 2.8*	4.59 ± 0.31*

Cells were maintained in the presence of culture medium alone (H, control HUVEC) or put in contact for 3 days with samples (*S* untreated stainless steel, *T* nitrided stainless steel, *SC* untreated, collagen coated stainless steel, *TC* nitrided, collagen coated stainless steel). LDH activity is expressed as μU/ml. Each value represents the mean ± SD of five (extracellular LDH) or three (intracellular LDH) separate experiments, each performed in triplicate. Intracellular/extracellular LDH ratio (intra/extra) is also reported

* $P < 0.01$ (in comparison with H); ** $P < 0.05$ (in comparison with H); ° $P < 0.05$ (in comparison with S and SC); ^ $P < 0.05$ (in comparison with T and TC)

Table 6 Effect of AISI 316L stainless steel sample types on proMMP-2 and MMP-2 release by HUVEC maintained in the presence of culture medium alone (H, control HUVEC) or put in contact for 3 days with samples

Sample type	proMMP-2	MMP-2
S	149 ± 13*	140 ± 7*
T	133 ± 19*	123 ± 9*
SC	145 ± 2*	108 ± 8°,^^
TC	131 ± 2*,°	95 ± 9°,^

Densitometric analysis of proMMP-2 and MMP-2 was carried out. MMPs levels were normalized with basis on cell proliferation. Data are given relative to control (H) set equal to 100. Each value represents the mean ± SD of six separate experiments

S untreated stainless steel, *T* nitrided stainless steel, *SC* untreated, collagen coated stainless steel, *TC* nitrided, collagen coated stainless steel

* $P < 0.01$ (in comparison with H); ° $P < 0.01$ (in comparison with S); ^ $P < 0.01$ (in comparison with T); ^^ $P < 0.05$ (in comparison with T)

intracellular levels are lower, in comparison with control HUVEC, when the cells were cultured in the presence of T or SC or TC samples.

The intra/extra LDH ratio is higher when HUVEC were maintained in the presence of culture medium alone (H) in comparison with the cultures in which the samples were present. Among the different samples only SC induces an intra/extra LDH ratio significantly lower than that registered when the nitrided samples (collagen coated or not, T and TC) were present.

3.8 Secretion of metalloproteinases

As HUVEC were found to constitutively express proMMP-2, the gelatinolytic activity of proMMP-2 and MMP-2 was determined in the culture medium of HUVEC maintained for 3 days in the absence or in the presence of the studied samples. Since in the culture medium FBS, which contains endogenous MMPs, was present, the gelatinolytic activity of the culture medium alone was registered and detracted from that shown by HUVEC incubated or not with the samples under study. The densitometric values were calculated, normalized with basis on cell proliferation, and reported in Table 6 as per cent of those of HUVEC maintained in the culture medium alone (H). ProMMP-2 gelatinolytic activity always shows a significant increase in comparison with control HUVEC, while a decrease with respect to the untreated samples (S) is registered in the presence of the surface treated and collagen coated samples (TC). The increase in MMP-2 is significant, in comparison with control HUVEC, only in the presence of samples S or T, while, when these samples were collagen coated, the gelatinolytic activity is lower in comparison with the collagen uncoated samples (S and T). ProMMP-9 and MMP-9 levels are very low, and a densitometric analysis was not always feasible (data not shown). However, an increase in proMMP-9 in comparison with control HUVEC is registered, particularly accentuated in the presence of samples S. MMP-9 gelatinolytic activity is always higher with respect to control cells, but it shows a tendency to decrease when HUVEC were maintained in contact with collagen coated samples. The lowest value is obtained in the presence of surface treated and collagen coated samples (TC).

4 Discussion

Low temperature nitriding of austenitic stainless steels has received increasing attention in the last years for enhancing wear and corrosion resistance of these alloys [23], but few studies have been focused on the effects of this treatment on the biocompatibility [39–43]. Moreover, in the international literature there is a lack of information on the possibility of using low temperature nitrided austenitic stainless steels as substrate for bioactive protein coatings.

In the present study low temperature nitriding was carried out on AISI 316L austenitic stainless steel by means of the glow-discharge nitriding technique. The peculiar structure of the nitrided surface, observed by many authors [24, 28, 31, 32], is hypothesized to be due not only to plasma etching, but also to local plastic deformation. Plastic deformation may occur during the formation of the modified surface layers owing to the high internal stresses caused by nitrogen solubilisation. This fact is supported

also by the presence of the small slip lines which are observable near the surface when the cross-section of the nitrided samples are examined. The slip bands, delineated within austenitic grains, and the high reliefs at grain boundaries contribute to slightly increase the average surface roughness of the nitrided samples. The main constituent of the modified surface layers is the S phase, the supersaturated interstitial solid solution of nitrogen in the expanded and distorted f.c.c. lattice. X-ray diffraction analysis shows also the presence of small amounts of nitrogen induced h.c.p. martensite, ε'_N. It may be supposed that this phase forms from the f.c.c. γ-Fe phase due to the effects of the solubilised nitrogen, which is able not only to induce high internal stresses, as previously recalled, but also to decrease the stacking fault energy of the steel, promoting martensite formation [24, 44].

Low temperature nitriding allows not only to increase the surface microhardness of AISI 316L, but also to enhance its corrosion resistance, as shown by polarization measurements and EIS analysis. In particular, polarization measurements, performed potentiodinamically on untreated and nitrided samples in PBS solution, show that nitrided samples have higher corrosion potential values and lower passive currents in respect of the untreated alloy, in accordance with the enhancement of corrosion resistance in chloride-ion containing solutions usually observed when modified surface layers, mainly consisting of S phase, are able to form [23, 24]. On the other hand, the potential values, at which a passive-transpassive transition occurs, are comparable for the two sample types. When tests are performed in NaCl aqueous solutions, the corrosion resistance of low temperature nitrided samples usually shows a more marked increase in respect of that of the untreated alloy. As an example, when nitrided samples, treated with the same experimental parameters used in the present study, are tested in a 5 % NaCl aerated solution, they show not only higher corrosion potential and lower passive current values, but also have a pitting potential [$>$ +1,000 mV (Ag/AgCl)] which is significantly higher than that of untreated AISI 316L [+775 mV (Ag/AgCl)] [45]. It may be hypothesised that the comparable pitting potential values, observed for untreated and nitrided samples tested in PBS, may be due to anodic inhibitor effects of the phosphates present in the PBS solution, which may be adsorbed to the stainless steel surface and form a film on it, so that the interaction between the passive film and the corrosive solution is decreased and the pitting initiation is delayed [35, 46].

In order to minimize the possible effects of sterilization of the samples under study, we have chosen to follow the procedure reported by Yuan et al. [9] for AISI 316L stainless steel samples, avoiding the autoclaving at 120 °C. In fact, even if the thickness of the surface oxide layer of AISI 316L samples increases by autoclaving [47], contributing to the higher corrosion resistance of the autoclaved samples than polished, non-autoclaved ones, we have preferred to avoid the influence of the autoclaving sterilization method on the surface of the metallic samples under study, in order to better evaluate the well defined treatments applied, i.e. nitriding and collagen coating.

In the present study collagen coating was performed on both untreated and nitrided samples without the use of chemical pre-treatments, which are usually employed in order to allow a good adhesion of collagen on metal alloys [13, 19, 20]. Plasma pre-treatment of AISI 316L has demonstrated to be also an efficient method for favouring collagen coating [18]. Without the use of a surface pre-treatment, the collagen adhesion is poor, as observed in the present study and by Hauser et al. [18]. The nitriding treatment results to be able to promote the adhesion of collagen-I, and it may be hypothesized that, for this result, both surface roughness and surface condition of the nitrided samples play a role.

Human cell cultures have been widely used to verify biocompatibility, and HUVEC in particular have been employed, besides us [39, 48], by many researches. Yeh et al. [10] demonstrated that the phenotypic feature of HUVEC, including growth, expression of proteins, and intercellular contact were altered when the cells were grown on a metallic surface, but such parameters varied widely according to the metals tested. Shahryari et al. [49] registered the attachment of HUVEC on the unmodified and cyclic potentiodynamic passivated AISI 316LS surface after 0.5–4 h, but no significant differences between the surfaces were identified for any of the incubation periods. In the same manner, we have not found any significant variation among the different sample types, when HUVEC proliferation was registered after 4-h incubation. On the other hand, differences in cell proliferation were reported by Shahryari et al. [49] after 2-, 7-, 11-day incubation. In our research HUVEC proliferation significantly changes after 3- or 5-day incubation. In particular, after 5-day incubation HUVEC show the best growth on the nitrided and collagen coated samples (TC), suggesting that these surface treatments of AISI 316L stainless steel may be favourable for endothelial cell proliferation. An enhanced endothelial cell growth on coated metals was also observed by Waterhouse et al. [12] with recombinant human tropoelastin and by Chen et al. [19, 20] with heparin and collagen. Chen et al. [19, 20] quantified the number of adherent platelets by determining the LDH release after lysis of the cells. We too assayed extracellular LDH, i.e. LDH released by HUVEC in the culture medium, and also intracellular LDH present in HUVEC lysates. We have chosen to assay LDH, as also Haslam et al. [50] estimated the number of viable animal cells based on their LDH

activities, and concluded that LDH determination is particularly useful for screening potential cell-growth inhibitors. Really, in our research, LDH assay confirms the results of HUVEC proliferation, indicating, however, that, when intra/extra LDH ratio is calculated, none treatment is able to restore control values, even if a lower negative influence of the nitrided and collagen coated or not samples (T and TC) is registered.

As regards the physiology and pathology of the vascular system, MMPs produced by endothelial cells are of particular interest. Therefore, those conditions that may affect their expression or activity must be taken into account. MMPs, in addition to degrade components of the extracellular matrix, exert many other physiological and pathophysiological roles [51, 52], their proteolytic activities being regulated by complex mechanisms at different levels (gene transcription and translation, post-translational modifications, endogenous inhibitors). MMP-2 is found in normal cardiomyocytes, as well in human arteries and in normal human vein endothelial cells. The expression of MMP-9 is first induced in response to pro-inflammatory cytokines, and is normally associated with activated leukocytes and macrophages and human endothelial cells [53]. Cavdar et al. [54] reported that HUVEC constitutively express only proMMP-2 at 72 kDa, whereas MMP-9 is undetected. Also Izidoro-Toledo et al. [55] found, always for HUVEC cultures, bands at 72 and 92 kDa, which correspond to the inactive form of MMP-2 and MMP-9, respectively, and were not able to detect the active forms of MMP-2 or MMP-9. Otherwise, we have detected both proMMP-2 and MMP-2, as confirmed by the use of a positive control.

Our findings have shown that, in response to the incubation of the HUVEC with the metallic samples under study, MMP-2 and MMP-9 remarkably increase in comparison with control cells, even if MMP-9 are very low, as also reported by Izidoro-Toledo et al. [55]. Since MMP-9 digests extracellular matrix molecules, such as gelatine, elastin, and collagen [56], we have verified whether a collagenolytic activity may be present in the culture medium of HUVEC. For this purpose we have carried out a zymography, in which instead of gelatin, type-I collagen was present, i.e. the same collagen used to coat AISI 316L samples, in order to exclude that the collagen coating could be digested by MMP-9 released by HUVEC. Really, none collagenolytic activity was registered. On the contrary, the gelatinolytic activity of proMMP-2 and MMP-2 is well detectable. In particular, the increase in proMMP-2 levels suggests that newly formed proenzymes are rapidly secreted. The nitrided and collagen coated samples (TC) induce a significantly lower release of proMMP-2 in comparison with the untreated uncoated ones (S), but the protection of the collagen coating is evident when the gelatinolytic activity of MMP-2 is considered. In fact, in the presence of the collagen coated samples, MMP-2 levels are quite those of control cells, indicating that the collagen protection is effective in controlling the release of the active form of MMP-2. This result is, to our opinion, very important as it has been demonstrated that MMP-2 plays a significant role not only in the degradation of the extracellular matrix component, but also at the cardiomyocyte level. Alteration of extracellular matrix proteins by MMP-2 may cause perturbations in cell–cell adhesion and tissue integrity, while the degradation of essential components of the sarcomere by MMP-2 is responsible for contractile dysfunction. Moreover, the degradation products of these proteins may trigger autoimmune-like responses and subsequent inflammation cascades [57]. As MMPs are also implicated in the pathogenesis of acute myocardial inflammation [58], it is fundamental that a medical implant device, such as a stent, does not remarkably affect MMPs levels. So, any surface modification, which could lead to this result, is highly desirable.

5 Conclusions

Low temperature glow-discharge nitriding, performed at 400 °C, 5 hPa for 5 h, produces, on AISI 316L austenitic stainless steel, modified surface layers, consisting mainly of S phase. The nitrided samples show a marked increase of surface microhardness and an enhancement of corrosion resistance in PBS solution in comparison with the untreated alloy. Moreover, the nitriding treatment seems to promote the coating with collagen-I, without the use of chemical coupling agents, in respect of untreated AISI 316L stainless steel.

Biocompatibility tests were carried out in vitro putting in contact untreated and nitrided samples, coated or not with collagen, with endothelial cells (HUVEC) in culture. It is interesting to note that the proliferation of HUVEC present on the surface of the samples shows the highest value after 5-day incubation with the nitrided and collagen coated samples, suggesting that these treatments may be favourable for endothelial cell proliferation. The collagen protection is also effective in controlling the release of MMP-2, whose increase is significant, in comparison with control cells, in the presence of uncoated samples. It may be therefore concluded that the nitriding and collagen coating of AISI 316L stainless steel are treatments that improve, almost in part, the biocompatibility of endothelial cells.

Acknowledgments This study was supported by grants from MIUR (Ministero dell'Istruzione, dell'Università e della Ricerca) and by a donation of Ente Cassa di Risparmio di Firenze.

References

1. Wapner KL. Implications of metallic corrosion in total knee arthroplasty. Clin Orthop Relat Res. 1991;271:12–20.
2. Lo KH, Shek CH, Lai JKL. Recent developments in stainless steels. Mater Sci Eng R. 2009;65:39–104.
3. Jacobs AM, Gloff LM. Podiatric metallurgy and the effects of implanted metals on living tissues. Clin Podiatry. 1985;2:121–41.
4. Hallab N, Merritt K, Jacobs JJ. Metal sensitivity in patients with orthopaedic implants. J Bone Joint Surg Am. 2001;83-A:428–36.
5. Hallab N, Link HD, McAfee PC. Biomaterial optimization in total disc arthroplasty. Spine. 2003;28:139–52.
6. Santin M, Mikhalovska L, Lloyd AW, Mikhalovsky S, Sigfrid L, Denyer SP, Field S, Teer D. In vitro host response assessment of biomaterials for cardiovascular stent manufacture. J Mater Sci. 2004;15:473–7.
7. Hong J, Andersson J, Ekdahl KN, Elgue G, Axen N, Larsson R, Nilsson B. Titanium is a highly thrombogenic biomaterial: possible implications for osteogenesis. Thromb Haemostasis. 1999;82:58–64.
8. Joner M, Finn AV, Farb A, Mont EK, Kolodgie FD, Ladich E, Kutys R, Skorija K, Gold HK, Virmani R. Pathology of drug-eluting stents in humans: delayed healing and late thrombotic risk. J Am Coll Cardiol. 2006;48:193–202.
9. Yuan Y, Liu C, Yin M. Plasma polymerized *n*-butyl methacrylate coating with potential for re-endothelialization of intravascular stent devices. J Mater Sci Mater Med. 2008;19:2187–96.
10. Yeh H-I, Lu S-K, Tian T-Y, Hong R-C, Lee W-H, Tsai C-H. Comparison of endothelial cells grown on different stent materials. J Biomed Mater Res. 2006;76A:835–41.
11. Kushwaha M, Anderson JM, Bosworth CA, Andukuri A, Minor WP, Lancaster JR Jr, Anderson PG, Brott BC, Jun H-W. A nitric oxide releasing, self assembled peptide amphiphile matrix that mimics native endothelium for coating implantable cardiovascular devices. Biomaterials. 2010;31:1502–8.
12. Waterhouse A, Yin Y, Wise SG, Bax DV, McKenzie DR, Bilek MMM, Weiss AS, MKC Ng. The immobilization of recombinant human tropoelastin on metals using a plasma-activated coating to improve the biocompatibility of coronary stents. Biomaterials. 2010;31:8332–40.
13. Morra M, Cassinelli C, Cascardo G, Cahalan P, Cahalan L, Fini M, Giardino R. Surface engineering of titanium by collagen immobilization. Surface characterization and in vitro and in vivo studies. Biomaterials. 2003;24:4639–54.
14. Morra M. Biochemical modification of titanium surfaces: peptides and ECM proteins. Eur Cells Mater. 2006;12:1–15.
15. Rammelt S, Schulze E, Bernhardt R, Hanisch U, Scharnweber D, Worch H, Zwipp H, Biewener A. Coating of titanium implants with type-I collagen. J Orthop Res. 2004;22:1025–34.
16. Rammelt S, Illert T, Bierbaum S, Scharnweber D, Zwipp H, Schneiders W. Coating of titanium implants with collagen. RGD peptide and chondroitin sulphate. Biomaterials. 2006;27:5561–71.
17. Stadlinger B, Pilling E, Mai R, Bierbaum S, Berhardt R, Scharnweber D, Eckelt U. Effect of biological implant surface coatings on bone formation, applying collagen, proteoglycans, glycosaminoglycans and growth factors. J Mater Sci Mater Med. 2008;19:1043–9.
18. Hauser J, Koeller M, Bensch S, Halfmann H, Awakowicz P, Steinau H-U, Esenwein S. Plasma mediated collagen-I-coating of metal implant materials to improve biocompatibility. J Biomed Mater Res. 2010;94A:12–26.
19. Chen JL, Li QL, Chen JY, Chen C, Huang N. Improving blood-compatibility of titanium by coating collagen-heparin multilayers. Appl Surf Sci. 2009;255:6894–900.
20. Chen J, Chen C, Chen Z, Chen J, Li Q, Huang N. Collagen/heparin coating on titanium surface improves the biocompatibility of titanium applied as a blood-contacting biomaterial. J Biomed Mater Res. 2010;95A:341–9.
21. Lampman S. Introduction to surface hardening of steels. In: ASM handbook, vol 4. Materials Park: ASM International; 1997. pp. 259–67.
22. Bell T. Surface engineering of austenitic stainless steel. Surf Eng. 2002;18:415–22.
23. Dong H. S-phase surface engineering of Fe–Cr, Co–Cr and Ni–Cr alloys. Int Mater Rev. 2010;55:65–98.
24. Fossati A, Galvanetto E, Bacci T, Borgioli F. Improvement of corrosion resistance of austenitic stainless steels by means of glow-discharge nitriding. Corros Rev. 2011;29:209–21.
25. Stetler-Stevenson WG. Matrix metalloproteinases in angiogenesis: a moving target for therapeutic intervention. J Clin Investig. 1999;103:1237–41.
26. Nguyen M, Arkell J, Jackson CJ. Human endothelial gelatinases and angiogenesis. Int J Biochem Cell Biol. 2001;33:960–70.
27. Spinale FG. Matrix metalloproteinases: regulation and dysregulation in the failing heart. Circ Res. 2002;90:520–30.
28. Borgioli F, Fossati A, Galvanetto E, Bacci T, Pradelli G. Glow-discharge nitriding of AISI 316L austenitic stainless steel: influence of treatment pressure. Surf Coat Technol. 2006;200:5505–13.
29. Lutterotti L, Matthies S, Wenk H-R. Material analysis using diffraction (MAUD): a user friendly java program for Rietveld texture analysis and more. In: Szpunar JA, editor. Proceedings of the 12th international conference on textures of materials (ICOTOM-12), vol 1. Ottawa: NRC; 1999. pp 1599–604.
30. Kalogeris TJ, Kevil CG, Laroux FS, Coe LL, Phifer TJ, Alexander JS. Differential monocyte adhesion and adhesion molecule expression in venous and arterial endothelial cells. Am J Physiol. 1999;276:L9–19.
31. Singh V, Marchev K, Cooper CV, Meletis EI. Intensified plasma-assisted nitriding of AISI 316L stainless steel. Surf Coat Technol. 2002;160:249–58.
32. Xu X, Yu Z, Wang L, Qiang J, Hei Z. Phase depth distribution characteristics of the plasma nitrided layer on AISI 304 stainless steel. Surf Coat Technol. 2003;162:242–7.
33. Shahryari A, Omanovic S, Szpunar JA. Enhancement of biocompatibility of 316LVM stainless steel by cyclic potentiodynamic polarization. J Biomed Mater Res. 2008;89A:1049–62.
34. Abreu CM, Cristóbal MJ, Merino P, Nóvoa XR, Pena G, Pérez MC. Electrochemical behaviour of an AISI 304L stainless steel implanted with nitrogen. Electrochem Acta. 2008;53:6000–7.
35. Valero Vidal C, Igual Muñoz A. Electrochemical characterisation of biomedical alloys for surgical implants in simulated body fluids. Corr Sci. 2008;50:1954–61.
36. Jiang S, Ma X, Sun Y, Sun M. Corrosion behaviour of AISI 302 steel treated by elevated temperature nitrogen plasma immersion ion implantation. Scripta Mater. 2005;53:1427–32.
37. Anandan C, William Grips VK, Ezhil Selvi V, Rajam KS. Electrochemical studies of stainless steel implanted with nitrogen and oxygen by plasma immersion ion implantation. Surf Coat Technol. 2007;201:7873–9.
38. Navarro-Flores E, Chong Z, Omanovic S. Characterization of Ni, NiMo, NiW and NiFe electroactive coatings as electrocatalysts for hydrogen evolution in an acidic medium. J Mol Catal A. 2005;226:179–97.
39. Martinesi M, Bruni S, Stio M, Treves C, Bacci T, Borgioli F. Biocompatibility evaluation of surface-treated AISI 316L austenitic stainless steel in human cell cultures. J Biomed Mater Res. 2007;80A:131–45.
40. Bordji K, Jouzeau J-Y, Mainard D, Payan E, Delagoutte J-P, Netter P. Evaluation of the effect of three surface treatments on the biocompatibility of 316L stainless steel using human differentiated cells. Biomaterials. 1996;17:491–500.

41. Arslan E, Iğdil MC, Yazici H, Tamerler C, Bermek H, Trabzon L. Mechanical properties and biocompatibility of plasma-nitrided laser-cut 316L cardiovascular stents. J Mater Sci. 2008;19:2079–86.
42. Buhagiar J, Bell T, Sammons R, Dong H. Evaluation of the biocompatibility of S-phase layers on medical grade austenitic stainless steels. J Mater Sci. 2011;22:1269–78.
43. Lin Y-H, Lan W-C, Ou K-L, Liu C-M, Peng P-W. Hemocompatibility evaluation of plasma-nitrided austenitic stainless steels at low temperature. Surf Coat Technol. 2012;206:4785–90.
44. Lei MK. Phase transformations in plasma source ion nitrided austenitic stainless steel at low temperature. J Mater Sci. 1999; 34:5975–82.
45. Borgioli F, Fossati A, Raugei L, Galvanetto E, Bacci T. Low temperature glow-discharge nitriding of stainless steels. In: Proceedings of the 7th European stainless steel conference—science and market, 21–23 Sept 2011, Como, Associazione Italiana di Metallurgia, Milano, 2011(CD-rom; ISBN: 978-88-85298-84-2).
46. Yau YH, Yang K, Zhang B. Pitting corrosion resistance of La added 316L stainless steel in simulated body fluid. Mater Lett. 2007;61:1154–7.
47. Hanawa T, Hiromoto S, Yamamoto A, Kuroda D, Asami K. XPS Characterization of the surface oxide film of 316L stainless steel samples that were located in quasi-biological environments. Mater Trans. 2002;43:3088–92.
48. Bruni S, Martinesi M, Stio M, Treves C, Bacci T, Borgioli F. Effects of surface treatment of Ti-6Al-4V titanium alloy on biocompatibility in cultured human umbilical vein endothelial cells. Acta Biomater. 2005;1:223–34.
49. Shahryari A, Azari F, Vali H, Omanovic S. The response of fibrinogen, platelets, endothelial and smooth muscle cells to an electrochemically modified SS316LS surface: towards the enhanced biocompatibility of coronary stents. Acta Biomater. 2010;6:695–701.
50. Haslam G, Wyatt D, Kitos PA. Estimating the number of viable animal cells in multi-well cultures based on their lactate dehydrogenase activities. Cytotechnology. 2000;32:63–75.
51. Yan C, Boyd DD. Regulation of matrix metalloproteinase gene expression. J Cell Physiol. 2007;211:19–26.
52. Chow AK, Cena J, Schulz R. Acute actions and novel targets of matrix metalloproteinases in the heart and vasculature. Br J Pharmacol. 2007;152:189–205.
53. Ho FM, Liu SH, Lin WW, Liau CS. Opposite effects of high glucose on MMP-2 and TIMP-2 in human endothelial cells. J Cell Biochem. 2007;101:442–50.
54. Cavdar Z, Oktay G, Egrilmez MY, Genc S, Genc K, Altun Z, Islekel H, Guner G. In vitro reoxygenation following hypoxia increases MMP-2 and TIMP-2 secretion by human umbilical vein endothelial cells. Acta Biochim Pol. 2010;57:69–73.
55. Izidoro-Toledo TC, Guimaraes DA, Belo VA, Gerlach RF, Tanus-Santos JE. Effects of statins on matrix metalloproteinases and their endogenous inhibitors in human endothelial cells. Naunyn-Schmied Arch Pharmacol. 2011;383:547–54.
56. Nagase H, Visse R, Murphy G. Structure and function of matrix metalloproteinases and TIMPs. Cardiovasc Res. 2006;69:562–73.
57. Goser S, Andrassy M, Buss SJ, Leuschner F, Volz CH, Otti R, Zittrich S, Blaudeck N, Hardt SE, Pfitzer G, Rose NR, Katus HA, Kaya Z. Cardiac troponin I but not cardiac troponin T induces severe autoimmune inflammation in the myocardium. Circulation. 2006;114:1693–702.
58. Li YY, McTiernan CF, Feldman AM. Proinflammatory cytokines regulate tissue inhibitors of metalloproteinases and disintegrin metalloproteinase in cardiac cells. Cardiovasc Res. 1999;42:162–72.